Evaluation of CFD as a Surrogate for Mach 2.4 to 4.6 Wind-Tunnel Testing – Project Overview

James C. Ross[1]
NASA Ames Research Center, Moffett Field, CA, 94035, USA

Matthew N. Rhode[2], Bryan Falman[3], Karl T. Edquist[4], Mark Schoenenberger[5], Gregory J. Brauckmann[6], Bil L. Kleb[7], Thomas K. West[8], Stephen J. Alter[9], David W. Witte[10]
NASA Langley Research Center, Hampton, VA, 23681, USA

The debate over when wind-tunnel testing will be replaced by Computational Fluid Dynamics (CFD) comes and goes. More recently the debate has subsided with a more collaborative spirit between practitioners of these two disciplines resulting in significant improvements in the outcomes of both. There may come a time, however, when CFD has sufficient accuracy to supplant WTT as the dominant or perhaps only tool for aerodynamic simulation. If and/or when that happens, financial pressures favor efforts to close or severely limit the operations of wind tunnels. Presumably additional resources will go toward CFD to generate aerodynamic databases, load environments, and new aero/fluid-dynamic knowledge. It is therefore important to develop appropriate processes by which wind-tunnel closure decisions are made to ensure that facilities critical to industry and government research and development aren't closed prematurely without proof that the available CFD tools have sufficient accuracy and low-enough cost (and enough experts and computational facilities) to take on the traditional role of wind tunnels. This paper will describe a project intended to answer the specific question of whether CFD can replace wind-tunnel testing for the limited Mach-number range 2.4 to 4.6. The project involves wind-tunnel testing and coordinated CFD for a variety of vehicle and flow-physics types in the high-speed leg of the Unitary Plan Wind Tunnel at NASA's Langley Research Center.

I. Nomenclature

LUPWT	=	Langley Unitary Plan Wind Tunnel
L_{ref}	=	model reference length
C_p	=	pressure coefficient
CA	=	force coefficient in the (model) axial direction
CN	=	force coefficient in the (model) normal direction

[1] Aerospace Engineer, Experimental Aerophysics Branch, AIAA Associate Fellow.
[2] Research Engineer, Aerothermodynamics Branch, AIAA Senior Member.
[3] Lead Engineer, Jacobs Technology, Inc.
[4] Research Engineer, EDL Technology Branch, AIAA Associate Fellow.
[5] Research Engineer, EDL Technology Branch, AIAA Senior Member.
[6] Research Engineer, Aerothermodynamics Branch, AIAA Associate Fellow.
[7] Senior Researcher, Aerothermodynamics Branch, AIAA Associate Fellow.
[8] Research Engineer, E401, AIAA Member.
[9] Research Engineer, Aerothermodynamics Branch, AIAA Senior Member.
[10] Research Engineer, D306, AIAA Senior Member.

II. Introduction

In 2012, the Unitary Plan Wind Tunnel at NASA's Langley Research Center (LUPWT) was mothballed and placed on the demolition list with a target date of 2022. At the time, the demand for data in the high-supersonic speed range was low, particularly for NASA projects. The cost to NASA projects for running tests in all NASA wind tunnels was also very high then, suppressing demand for the facility. In the years since, the facility has been mothballed for several months at a time, operated by Jacobs Engineering under a full-cost recovery model with no investment in upgrades or improvements, and eventually recertified and reopened as a NASA facility, temporarily, to perform important aerodynamic testing for the Space Launch System. It remains on the demolition list for 2022, however, despite a recent increase in demand for testing in the facility.

In 2018 NASA began a study to evaluate the current ability of Computational Fluid Dynamics (CFD) to reliably predict a wide variety of flow fields associated with vehicles of interest to NASA and the Department of Defense in the Mach 2.4 to 4.6 range. The results of this study will provide a measure of the risk associated with abandoning the facility, which is unique in the NASA inventory – the high-speed leg of the facility is one of only two continuous flow wind tunnels in the US that operates at high supersonic speeds. This CFD Evaluation Project was undertaken by the NASA Aerosciences Evaluation and Testing Capability (AETC) to identify the technical risks to NASA and national programs that might result from relying solely on CFD for aerodynamic data in the Mach 2.4 to 4.6 range.

In addition to the technical risks, the potential financial risks of eliminating a facility in favor of computational simulations need to be addressed. We will be estimating the cost of generating a database solely from CFD and the computational resources required to replace the wind tunnel as a source of. Without a wind tunnel, additional resources (high-performance computing hardware and experienced CFD practitioners) will be required to produce the quantity of data acquired in the wind tunnel on a continuing basis.

III. Evaluation Ground Rules

Each of the evaluation teams followed a similar set of processes to reduce any variability that might increase the difficulty in understanding the results. After selecting the geometry and the configuration or flow variables to be examined, the wind-tunnel model design and refinement of the geometry definition to facilitate.

A. CFD Rules

In general, the wind-tunnel and CFD practitioners on the evaluation teams worked collaboratively. The exception was when the wind-tunnel data could be shared. There were two phases of CFD that we wanted to include in each evaluation: pre-test computations that would be done without any knowledge of the wind-tunnel results and post-test computations that would incorporate any lessons learned from the comparisons of the CFD and wind-tunnel results. The post-test computations also provided valuable insight into puzzling results from the wind-tunnel tests, highlighting that wind-tunnel testing and CFD are often very complimentary providing increased value when performed together). It wasn't always possible to complete the pre-test computations before the start of the wind-tunnel test, so the data was not released to the full team until all the pre-test computations were completed.

The pre-test CFD was intended to look at a broad set of test conditions, model configurations, and propulsion-system parameters that encompassed the important flow physics for each evaluation. These variations included Mach number, Reynolds number, control-surface deflections, nozzle size and locations, relative position of model components, and thrust levels, where appropriate. The number of comparison cases varied from six to over 400.

B. Data Comparisons and Uncertainty Quantification

Each team had their own priorities for what comparisons to make between the CFD and wind-tunnel results. Each had different challenges in what could be measured in the wind tunnel and what measurements were the most important for their projects. The selected data comparisons were noted in the descriptions of each of the evaluation teams, but the uncertainty quantification process was intended to be common for all the teams. Since the wind-tunnel data system does not include uncertainty as a standard data product, and some of the evaluation teams were using data acquired in tests conducted long before this project started, each team came up with their own measurement uncertainties, all based on established techniques. Hubbard and Houlden [1] describe the methodology used to develop the measurement uncertainties for the empty tunnel flow characterization. In this case, the systematic measurement uncertainty was determined using Monte Carlo uncertainty propagation and the random uncertainty from a statistical analysis of the repeat wind-tunnel data. For some of the teams, the systematic measurement uncertainty was determined using the current AIAA standard methodology [2].

For the comparisons with the CFD results, the teams are following the process outlined by Baurle and Axdahl [3] In this approach, CFD is used to model selected experimental uncertainties that aren't captured by the experimental uncertainty, for example the relative position of the boosters to the core of the SLS model.

A. Costs

Each team kept track of their costs throughout the evaluation process. The largest cost during the preparation phase of each evaluation was labor, whether for model design and fabrication or the geometry preparation, grid generation, and best-practices development for the CFD work. In many cases, CFD was used in designing the wind-tunnel models. In particular, the internal flow paths of the models made good use of CFD to minimize pressure losses and to improve flow uniformity for the high-pressure air simulations of propulsion systems. This cost was book kept with the wind-tunnel model development. Table 1 shows an example of the cost breakdown associated with the wind tunnel testing.

Table 1 Cost breakdown for a typical wind-tunnel test.

Item	Labor or WT hours	Procurement	Total Cost, %	Evaluation Cost, %	Database Cost, %
Geometry Development					
Model design & fab management					
Model fabrication					
Test lead and other "customer" labor					
Special Instrumentation: PSP, etc.					
WT occupancy (Total)					
WT power (Total)					
WT occupancy (Evaluation)					
WT power (Evaluation)					
WT occupancy (Database)					
WT power (Database)					
		Total			
			Evaluation		
				Database	

Table 1 shows three cost summations for the total cost of the test, the cost of just the evaluation portion of the test, and the estimated cost of any database portion of the test. Since these tests were intended to provide value to the partner projects, there were typically a mix of model configurations and test conditions specifically for evaluating the CFD results and others for project-specific sensitivity studies or database development. The total cost of the testing performed during this study is captured as the Total cost in Table 1. The cost of performing a test that only included the specific conditions tested for the CFD evaluations is captured in the Evaluation cell, including all the "overhead" costs of preparing for and running a wind-tunnel test plus any special instrumentation used specifically for the CFD comparisons. The overhead costs also include model design and fabrication and the labor for the test lead and any additional labor that would be associated with a wind-tunnel customer (test engineers, data analysts, etc.).

Table 2 shows the costs that were tracked for the CFD effort. The tasks were broken down to this level of detail to better understand where further automation or collaboration between mechanical designers would help decrease the labor costs. The average job wait in the que and the run times were included to gage the potential requirement for increased high-performance computing capacity to satisfy the computational needs should the LUPWT be removed from use. Those average times also help in estimating the cost of a database-building effort to compare with the cost of the wind-tunnel database test.

Table 2 Cost breakdown for the CFD efforts.

Name	Total Labor Hours	CAD – Geom. Prep.	CFD Best Practices	Grids	CFD Automation & Scripting	Managing CFD Jobs	Data Review & Reporting	Visualization & Understanding Data	UQ	Total SBU	Average Job Wait Time	Average Job Run Time, SBU
Totals:												

IV. Evaluation Teams

One requirement of the CFD Evaluation Project is that the CFD effort must be staffed and funded by a partner project. Each evaluation team lead was usually a participant in the partner project and funded by the partner project. Funding for the wind-tunnel testing was provided by AETC, the largest of which are the cost of the wind-tunnel model and the wind-tunnel test time. This ensured that the results generated serve more than the purpose of the CFD Evaluation Project. Five flow/vehicle types were selected by a group of NASA, industry, and DoD experts as requiring good understanding for vehicles under consideration either currently or in the foreseeable future. Two additional cases were adopted as well, flow characterization of the empty test section and a simple wing-body configuration used as the check standard model for the LUPWT. The empty test section case was added because all the other wind-tunnel tests and matching CFD would be run in the high-speed leg of the wind tunnel, and it had not been calibrated or characterized since 1981 [4]. The check standard model [5] was added because it represents a much easier vehicle configuration to compute and there was a large amount of data with which to compare the CFD results. The following sections describe the seven test cases selected and the associated difficult flow physics.

A. Test-Section Flow Characterization

The Unitary Plan Wind Tunnel at NASA's Langley Research Center (LUPWT) is a closed circuit, continuous flow, variable-density supersonic wind tunnel. It has two test sections, each measuring approximately 4 by 4 by 7 feet. Test section 2 has the higher Mach-number range of 2.3 to 4.6. By varying the total pressure tests can be performed at unit Reynolds number from approximately 0.5 to 8.25 million per foot. A complete description of the facility can be found in reference 4.

An accurate understanding of the flow in the test section is important not only as an evaluation case, but as an important input to all the other evaluation teams. To accurately predict the aerodynamics of a model in the wind tunnel, the flow in the tunnel must be accurately modeled. The sliding block nozzle of the wind tunnel shown in Figure 1, results in a non-uniform velocity distribution in the test section simply because of the nozzle asymmetry. This was observed the earlier test-section calibration [4], and was likely expected to be the case by the designers of the wind tunnel in the 1950's. The asymmetric, sliding-block nozzle can provide a wide Mach number range with a very simple moving part and the price of that simplicity is a small vertical Mach-number gradient in the test section. Since the previous calibration had been performed decades ago, we adopted test-section flow characterization as the first evaluation case.

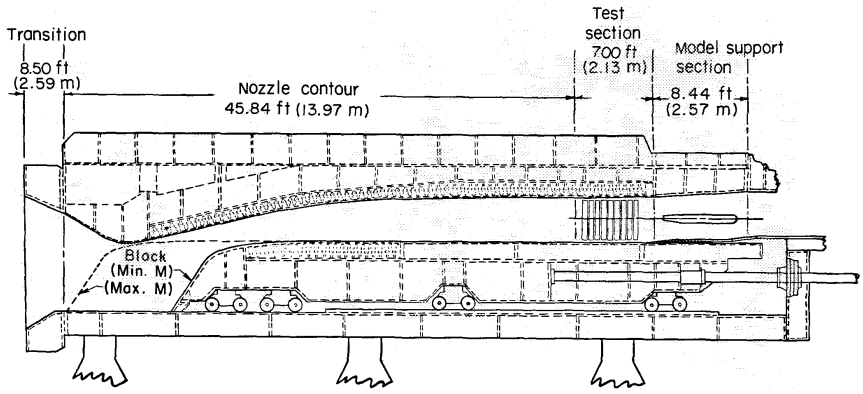

Fig. 1 Side view of high-speed test section of the UPWT [4].

Several CFD codes were used to predict the flow in the test section at nine test conditions that formed the set of conditions for the other Evaluation Teams to investigate, if appropriate. The companion testing used a rake with 19 five-hole probes to document the flow in the test section. The rake was mounted on the traversing model support, with a resulting total of up to 1463 points measured in the test section per test condition. Some of the details of the flow characterization testing are given by Childs, et al [6] and Hubbard and Houlden [1]

The CFD predictions were made using OVERFLOW [7], FUN3D [8], USM3D [9], STAR-CCM+ [10], and an adaptive-mesh version of FUN3D [11]. These represent a mix of commercial and government codes as well as codes using structured and unstructured grids. The computations encompassed the wind tunnel starting at the entrance to the settling chamber upstream of the nozzle section and extended through the test section with the simulations ending somewhat downstream of the model support.

Some omparisons of the CFD predictions with the measured flow in the test section are given by Childs, et al [6]. A discussion about the best practices developed for the predictions is also given. The flow predictions at, or just upstream of the start of the test section were used by the other evaluation teams as inflow boundary conditions to the test section, eliminating the need to simulate the full wind tunnel for every prediction of a model in the wind tunnel – a significant saving in computer time that was shown to not affect the predicted flow through the rest of the test section.

B. Supersonic Retro-Propulsion

Our partner project for the supersonic retro-propulsion evaluation team was the Game Changing Development Program which, among other topics, is studying new ways to deliver large, heavy payloads to Mars. The configurations chose for this study are the Hypersonic Inflatable Aerodynamic Decelerator (HIAD) [12, 13] and the Co-Optimization Blunt-body Re-entry Analysis Mid-L/D Rigid Vehicle (COBRA-MRV) [14, 15]. These vehicles are designed to deliver large payloads to the surface of Mars through a standard entry and descent down to a Mach number of around 2. At this point, further deceleration is provided by a retro-propulsion system which is used during the remainder of the descent down to a soft landing. Figure 2 shows the two vehicles and the conceptual entry, descent, and landing for both. Edquist, et al [16], describe detains of the planned test and the CFD analyses that are currently underway.

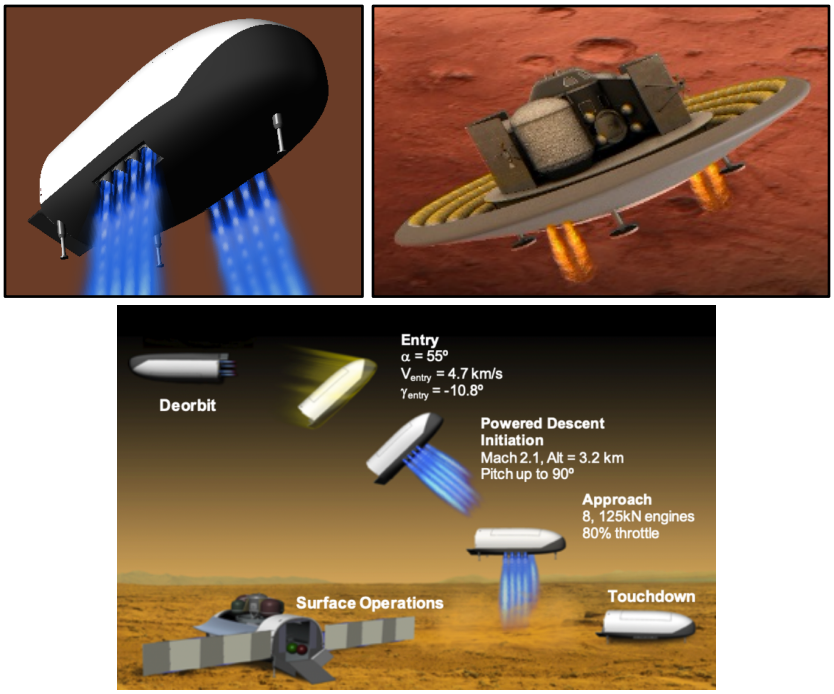

Fig. 2 HIAD and CobraMRV vehicles showing the proposed entry, unpowered and powered descent, and landing on Mars.

For this comparison study, the experimental data will consist primarily of temperature-corrected pressure-sensitive paint (PSP) measurements of the heat-shield pressure distribution. A Doppler Global Velocimetry (DGV) system is also being prepared for the test to measure flow in the plume and in the free-stream [17, 18]. Approximately 20 static-pressure taps on the heat shield of each model will allow anchoring of the PSP results to account for residual temperature effects and off-axis viewing and illumination angles. Figure 3 shows a cross-section through the HIAD model illustrating the flow path for the high-pressure air used to simulate the retro-rocket plumes in the wind tunnel. The CFD portion of the study includes a variety of codes: OVERFLOW, FUN3D, and LOCI-CHEM [19].

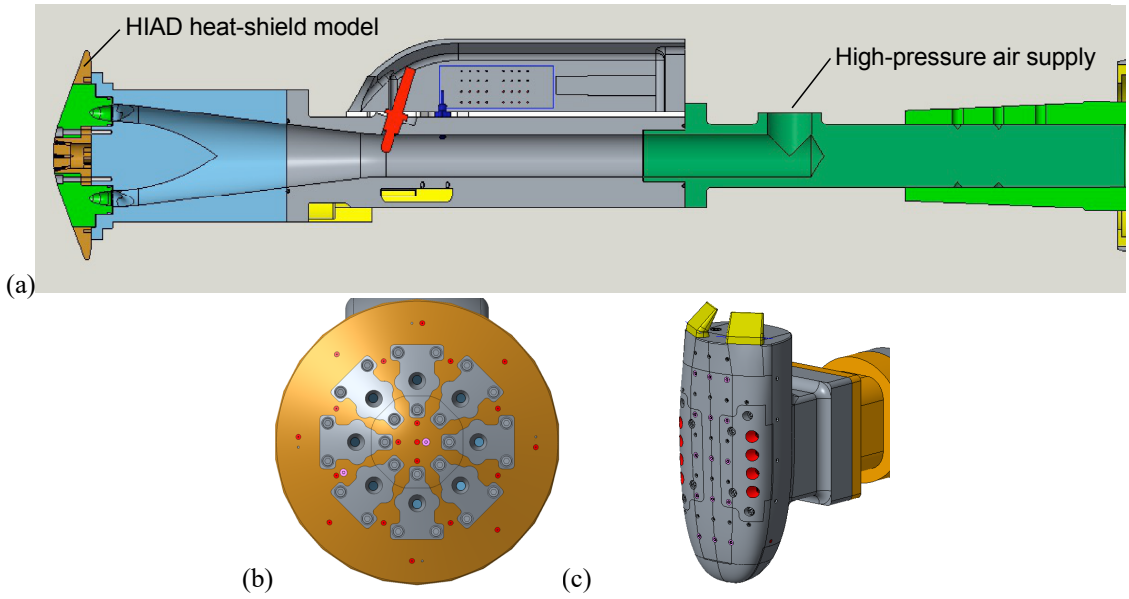

Fig. 3 HIAD and COBRA-MRV wind-tunnel models. (a) Cross section showing high-pressure-air flowpath. (b) HIAD model heat shield showing one nozzle arrangement. (c) COBRA-MRV model heat shield showing nozzle arrangement.

C. Hypersonic Vehicle Control-Surface Effectiveness

The CobraMRV briefly described in the previous section, employs a pair of body flaps for aerodynamic control during the initial phases of entry and descent. When the vehicle decelerates to Mach 2, further deceleration is provided by a retro-propulsion system which is used during the remainder of the descent down to a soft landing, as depicted in Figure 2. This evaluation team looked at the predictions of the effect of body flap deflections on the resulting aerodynamic forces and moments from Mach 4.6 down to 2.4 [20, 21].

The comparisons between results from CFD and experimental data were primarily for the model force and moment coefficients measured using an internal balance. The flap hinge moments were measured using hinge moment gages on each flap. In addition, the pressure distribution on the wind-tunnel model was measured using a combination of pressure-sensitive paint (PSP) and 60 standard static pressure taps. The two CFD codes used for the comparisons were Overflow and Fun3D with adaptive meshing.

Figure 4 shows the wind tunnel model in the wind tunnel and a close-up of the flap attachment to the hinge-moment gages. The pink color of the model in Figure 4b is the PSP as it looks in white light and Figure 4b shows the PSP when illuminated by the near ultra-violet lights that are used during data acquisition.

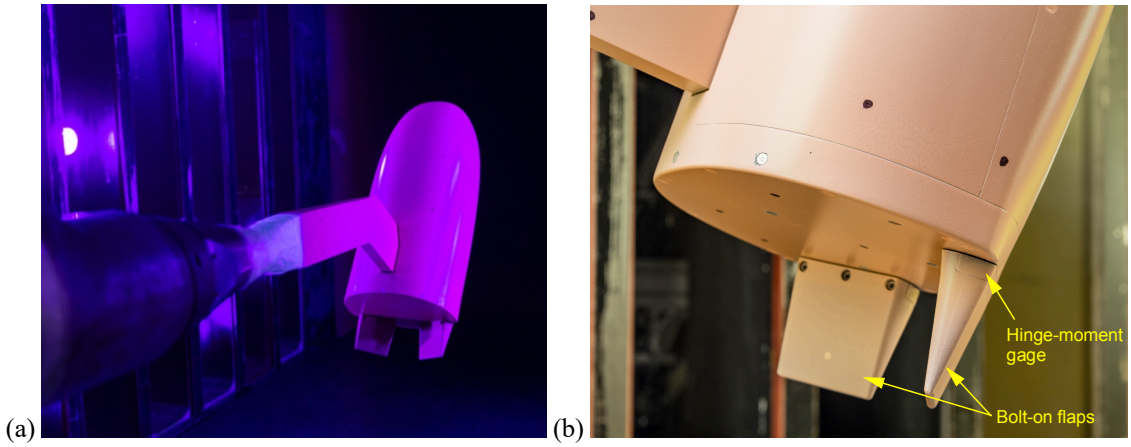

Fig. 4 Photographs of the wind-tunnel model: (a) in the wind tunnel and (b) a close-up of the body flaps and their attachment to the hinge-moment gages.

D. Hypersonic Inlet Integration and Performance

The pressure rise across a series of reflected shocks in the inlet duct is the mechanism by which the air ingested by a scramjet is compressed prior to mixing with the fuel and combusted. The total pressure rise is the limiting factor for the combustion-chamber pressure. Accurately predicting the pressure rise for an inlet-isolator for such engines has proven difficult which is the reason for including it as one of the evaluation cases. For this evaluation, partnered with the Hypersonic Technology Project, a wind-tunnel model of an inlet-isolator will be tested in the LUPWT and the results compared with the corresponding CFD predictions. A sketch of the model layout is shown in Figure 5. The model includes several moving surfaces to examine the effects on the overall performance and giving the CFD variations which will be compared with the experimental results.

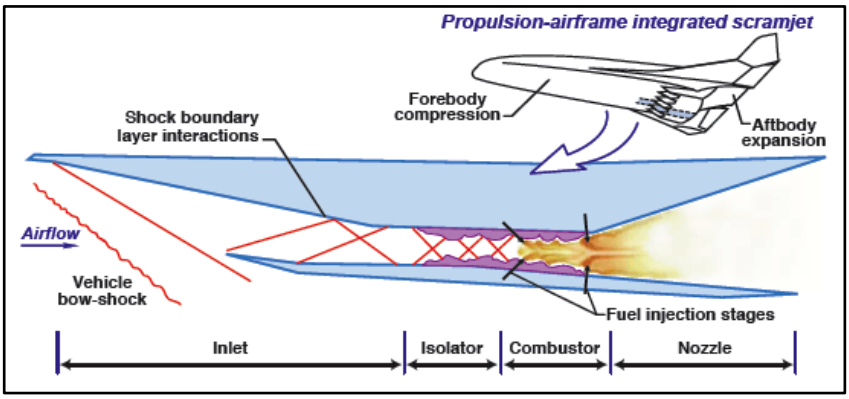

Fig. 5 Schematic representation of a hypersonic inlet and isolator.

Detailed pressure measurements will be acquired on the model upstream of the inlet and through the isolator and represent the primary comparisons between the wind-tunnel results and the CFD predictions. Several CFD methods will be part of the evaluation; VULCAN [22], LOCI-CHEM, FUN3D, Wind-US [23], and Kestrel [24].

E. Reaction Control System Jet Interactions

Another difficult to predict flow of major importance to NASA is the aerodynamic interaction between the reaction control system (RCS) plumes and the separated wake flow of entry bodies. These flows are part of the exploration probes that land on other planets and for crewed vehicles carrying astronauts as they return to Earth. The partner project for this evaluation is the Mars Sample Retrieval Lander [25]. The vehicle configuration is shown in Figure 6 along with a rendering of the wind tunnel model.

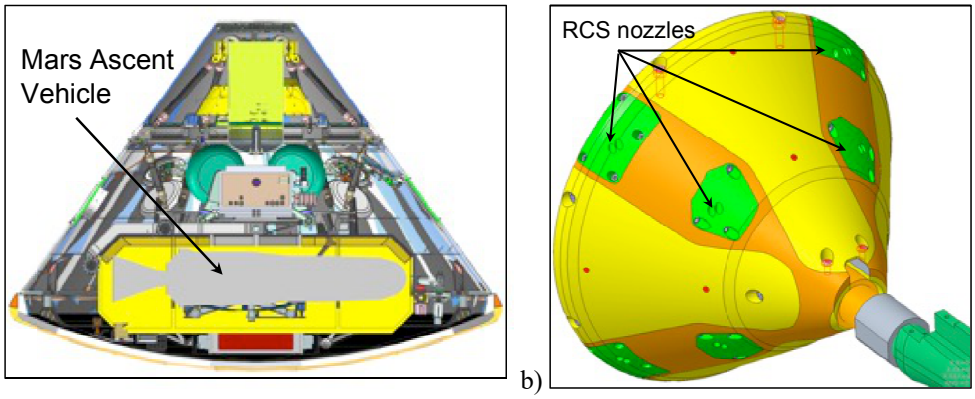

a) b)

Fig. 6 Mars Sample Retrieval Lander and the wind tunnel model to examine the RCS plume aerodynamic interactions. a) section cut through entry-descent vehicle showing the lander and Mars ascent vehicle stowed inside; b) wind tunnel model showing some of the interchangeable nozzle inserts.

The wind tunnel model will have several sets of nozzles, some of which will be used for the CFD evaluation while others will help the mission planners decide on a final configuration of RCS motors for the vehicle. The CFD predictions will be done using OVERFLOW and FUN3D. Comparisons will be made for the overall forces and

moments that will be measured using a flow-through internal balance and pressure distributions measured using a combination of static pressure taps and PSP. Schlieren images and possibly DGV measurements will also be acquired and add to the comparisons.

F. Multi-Body Separation - Space Launch System (SLS) Booster Separation

The SLS solid-rocket motors separate from the core stage at around Mach 4. Given the proximity of the boosters to the core stage and the relatively low thrust of the booster separation motors which provide the lateral acceleration of the boosters away from the core, the aerodynamic interactions generated during the separation event need to be well understood. Figure 7 shows a computational simulation of the booster separation. There are several flow features that must be well modeled including supersonic plumes downstream of the core-stage shock and interacting with the core stage, interactions of the booster shocks with the core and the separation motor plumes, and the effects of changing orientation of the boosters relative to the core stage.

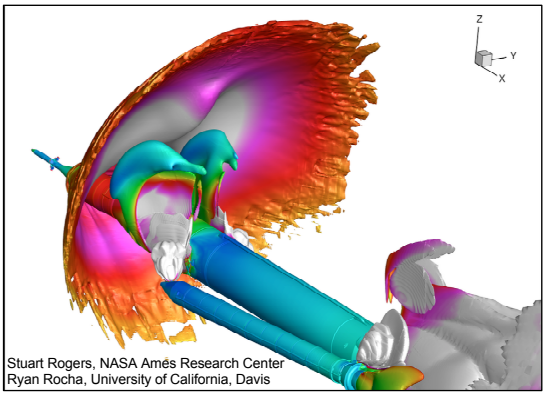

Fig. 7 Visualization of the SLS booster separation flow field predicted using OVERFLOW (https://www.nasa.gov/ames/image-feature/simulation-sls-booster-separation).

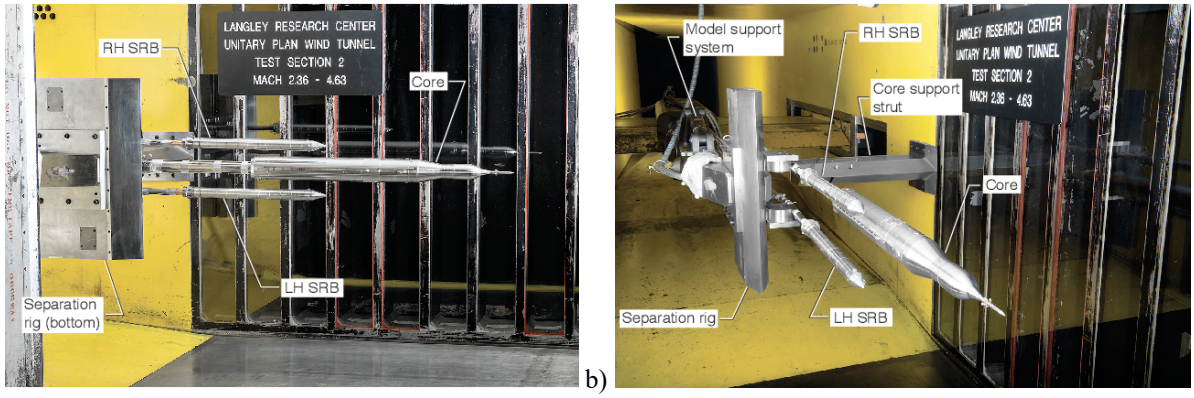

Fig. 8 Two views of the model and model support for the SLS booster separation testing performed at the LUPWT. a) Side view, b) view looking downstream

This evaluation did not require a new wind tunnel test. The SLS Program had run several booster-separation tests [26, 27]. We used this data for comparisons with new CFD results generated by a new CFD team that had no connection with the SLS CFD team and did not seek advice on how to run the simulations accurately. This gave us a fresh set of CFD solutions obtained on the same basis as the rest of the evaluation teams. Figure 8 shows the model and model support for the tests. To simulate, at least statically, the aerodynamics during separation, the model support could position the left- and right-hand solid rocket boosters (LH SRB and RH SRB, respectively) relative to the core stage. The booster-separation rocket motor plumes were simulated using high-pressure air. The model was instrumented with internal balances in the core and both boosters. The force and moment coefficients were the primary date used for comparisons with the CFD predictions which were performed using the LAVA [28] and FUN3D codes. PSP data acquired during the testing provided additional information for the comparisons.

G. Check Standard Model Aerodynamics

The check standard model was added to the list of evaluations to provide a case that should be relatively straightforward to compute the flow over. This is a model that is tested regularly to ensure that the wind tunnel measurements for this model show no significant change over time. This can help diagnose problems that may crop up with the data system or even changes in the flow quality. This model was originally built to study the transonic characteristics of an arrow-wing concept and the effects of leading- and trailing-edge flaps [5]. In its check-standard role, the model is tested with undeflected leading-and trailing-edge flaps. More than 15 of tests have been performed with this model, so we did not have to perform one for the evaluation work. A photograph of the model in the wind tunnel is shown in Figure 9.

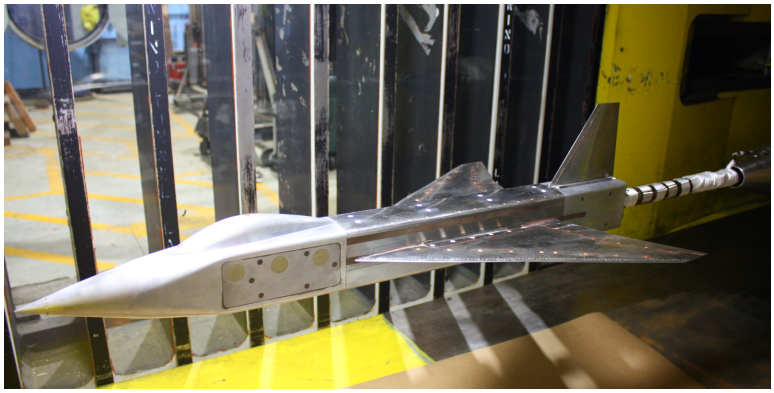

Fig. 9 LUPWT Check Standard model in mounted in the LUPWT high-speed test section.

The CFD predictions for this evaluation are from the LAVA and Kestrel CFD codes. Since this is the first time the flow over this configuration was predicted using CFD, a major task was simply digitizing the geometry from the original 1982 blueprints and recent laser scans.

V. Discussion

This Project will provide an important set of direct comparisons between the predicted and measured aerodynamics of several vehicle types in the simulated and real environment of the Langley Unitary Plan Wind Tunnel. The ability of CFD to predict these flows will be on input to a decision of whether to keep the LUPWT. The relative costs of CFD and wind-tunnel data will be an additional factor considered. This may represent the first time this kind of specific information will have been used as input to such a decision. While the Project is still in the data gathering stage with a few comparisons made so far. Preliminary comparisons are given in several companion papers [1, 6, 17, 18], giving perhaps a not-too-surprising indication of what the outcome of the evaluations may be.

References

[1] Hubbard, E. P. and Houlden, H. P., "Evaluation of CFD as a Surrogate for Wind-Tunnel Testing: Experimental Uncertainty quantification for the UPWT Flow Survey Test," AIAA Aviation Conference, August 2-6, 2021.

[2] "Standard: Assessment of Experimental Uncertainty with Application to Wind Tunnel Testing" (AIAA S-071A-1999), American Institute of Aeronautics and Astronautics, 1999.

[3] Baurle, R. A. and Axdahl, E. L., "Uncertainty Quantification of CFD Data Generated for a Model Scramjet Isolator Flowfield," JANNAF CS/APS/PSHS Joint Meeting, December 2017.

[4] Jackson, Jr., C. M., Corlett, W. A., and Monta, W. J., "Description and Calibration of the Langley Unitary Plan Wind Tunnel," NASA Technical Paper NASA TP-1905, NASA Langley Research Center, Langley Research Center, Hampton, VA, 1981.

[5] Riebe, G.D. and Fox, C.H., Jr., "Subsonic Maneuver Capability of a Supersonic Cruise Fighter Wing Concept,' NASA Technical Paper 2642, January 1987.

[6] Childs, R.E., Stremel, P.M., Hawke, V.M., Garcia, J.A., Kleb, W.L., Hunter, C., Parikh, P., Patel, M., Alter, S., and Salari, K., "Flow Characterization of the NASA Langley Unitary Plan Wind Tunnel, Test Section 2: Computational Results," AIAA Aviation 21 Conference, August 2021.

[7] Nichols, R.H., Trame, R.W, and Buning, P.G., "Solver and Turbulence Model Upgrades to OVERFLOW 2 for Unsteady and High-Speed Applications," AIAA Paper 2006-2824, June 2006.

[8] Biedron, R.T., et al, "FUN3D Manual: 12.7," NASA TM 2015-218761, May 2015.

[9] Frink,N.T., Pirzadeh, S.Z, Parikh, P.C., Pandya, M.J., and Bhat, M.K., "The NASA Tetrahedral Unstructured Software System," The Aeronautical Journal, Vol. 104, No. 1040, October 2000, pp. 491-499.

[10] Zastawny, M, and Lardeau, S., "Application of Simcenter STAR-CCM+ for Assessment of the Impact of CFD Modelling Approach in NASA Juncture Flow Simulations," AIAA Paper 2020-2736, AIAA Aviation Forum, June 15-19, 2020, Virtual Event.
[11] Kleb, W., Schoenenberger, M., Korzun, A., and Park, M., "Sketch-to-Solution: A case Study in RCS Aerodynamic Interaction," AIAA Paper AIAA2020-0673, AIAA Scitech 2020 Forum, Orlando, FL, 2020.
[12] Hughes, S.J., Cheatwood, F.M., Dillman, R.A., Wright, H.S., DelCorso, J.A., and Calomino, A.M., "Hypersonic Inflatable Aerodynamic Decelerator (HIAD) Technology Development Overview," AIAA Paper 2011-2524, 21st AIAA Aerodynamc Decelerator Systems Technology Conference and Seminar, May 23-27, 2011, Dublin, Ireland.
[13] Percy, T.K., Polsgrove, T., Sutherlin, S., Cianciolo, A.D., "Human Mars Entry, Descent and Landing Architecture Study: Descent Systems," AIAA Paper 2018-5193, 2018 AIAA Space and Astronautics Forum and Exposition, Sept. 17-19, 2018, Orlando, Florida.
[14] Garcia, J. A., Brown, J. L., Kinney D. J., Bowles, J. V., Huynh L. C., Jiang X.J., Lau E., Dupzyk, I. C., "Co-Optimization of Mid Lift to Drag Vehicle Concepts for Mars Atmospheric Entry," 10th AIAA/ASME Thermophysics Conference, 2010.
[15] Calderon, D., Sostaric, R.R., Garcia, J.A., Bowles, J.V., Kinney, D.J., Gaytan, C., Newton, H., Amar, J., and Wiens, Z., "Structural Mass Optimization with Manifest Packaging, and Outer Mold Line Updates of a Rigid Mid Lift-to-Drag Mars Entry Lander Vehicle", AIAA SciTech Form 2020, Orlando, FL, AIAA 2020-1509.
[16] Equist, K.T., Korzun, A.M., Kleb, B., Hawke, V.M., Rizk, Y.M., Olsen, M.E., and Canabal F., "Model Design and Pre-Test CFD Analysis for a Supersonic Retropropulsion Wind Tunnel Test," AIAA Paper 2020-2230, AIAA Scitech 2020 Forum, January 6-10, 2020, Orlando, Florida.
[17] Burns, R. A., Fahringer, T. W., and Danehy, P. M., "Velocity Measurements Across an Oblique Shock Using Pulse-Burst Cross-Correlation DGV," AIAA Scitech 2021 Forum, January 2021, Virtual Event.
[18] Acharya, A. S., Lowe, K. T., Ng, W.F., and Danehy P. M., "Particl Seeding Method for Small-Scale, High-Pressure Nozzles,", AIAA Paper 2021-1068, AIAA SciTech Forum, January 11-21, 2021, Virtual Event.
[19] Luke, E., "On Robust and Accurate Arbitrary Polytope CFD Solvers," AIAA Paper 2007-3956, June 2007.
[20] Ross, J. C., Denison, M. F., Childs, R. C., Garcia, J. A., Stremel, P. M., Hawke, V. M., Spooner, H. R., Reed, M. A., Kleb, B. L., Watkins, A. N., Danehy, P. M., Burns, T. W., Borg, S. E., and Robinson, P. E., "Evaluation of CFD for Simulation of High-Supersonic Control-Surface Effectiveness," AIAA Aviation Conference, August 2-6, 2021.
[21] Denison, M. F., et al, "Evaluation of CFD Predictions of CobraMRV Control Surface Effectiveness at the NASA Langley Unitary Plan Wind Tunnel," AIAA Aviation 21 Conference, August 2021.
[22] White, J., Baurle, R., and Nishikawa, H., "A 3-D Nodal-Averaged Gradient Approach For Unstructured-Grid Cell-Centered Finite-Volume Methods For Application to Turbulent Hypersonic Flow," AIAA Paper No. 2020-0652, Jan. 2020.
[23] Geogiadis, J. J., Yoder, D. A., Towne, C. S., Engblom, W. A., Bhagwandin, V. A., Power, G. D., Lankford, D. W., and Nelson, C. C., "Wind-US Code Physical Modeling Improvements to Complement Hypersonic Testing and Evaluation," AIAA Paper 2009-193, AIAA Aerospace Sciences Meeting, January 5-8, 2009, Orlando, Florida.
[24] McDaniel, D. R. and Morton, S. A., "HPCP CREAT -AV Kestrel Architecture, Capabilities and Future Directions," AIAA Paper 2018-0025, AIAA SciTech Forum, January 8-12, 2018, Kissimmee, Florida.
[25] Ivanov, M. C. and Sell, S. W., "Challenges of Mars Sample Return Lander Entry, Descent, and Landing," AAS Paper 20-106, American Astronautical Society Guidance Navigation and Control Conference, January 30 – February 5, 2020, Colorado Springs, Colorado.
[26] Winski, C. S., Danehy, P. M., Watkins, A. N., Shea, P. R., Meeroff, J. G., Lowe, K. T., Houlden, H. P., "Space Launch System Booster Separation Supersonic Powered Testing with Surface and Off-body Measurements," AIAA paper 2019-3505, AIAA Aviation 2019 Forum, June 17-21, 2019, Dallas, Texas.
[27] Wilcox, J. J., Pinier, J. T., Chan, D. T., and Crosby, W. A., "Space Launch System Booster Separation Aerodynamic Testing in the NASA Langley Unitary Plan Wind Tunnel," AIAA Paper 2016-0796, AIAA SciTech Forum, January 4-8, 2016, Sand Diego, California.
[28] Moini-Yekta, S., Barad, M. F., Sozer, E., Brehm, C., Housman, J. A., and Kiris, C. C., "Verification and Validation Studies for the LAVA CFD Solver," AIAA Paper 2-13-2448, 21st AIAA Computational Fluid Dynamics Conference, June 24-27, 2013, San Diego, California.